BLED WORKSHOPS
IN PHYSICS
VOL. 5, NO. 1

Proceedings of the Mini-Workshop
Quark Dynamics *(p. 62)*
Bled, Slovenia, July 12-19, 2004

Calculation of electroproduction amplitudes in the K-matrix formalism*

B. Golli[a,b], P. Alberto[c,e], L. Amoreira[d,e], M. Fiolhais[c,e], and S. Širca[f,b]

[a] Faculty of Education, University of Ljubljana, 1000 Ljubljana, Slovenia
[b] J. Stefan Institute, 1000 Ljubljana, Slovenia
[c] Department of Physics, University of Coimbra, 3004-516 Coimbra, Portugal
[d] Department of Physics, University of Beira Interior, 6201-001 Covilhã, Portugal
[e] Centre for Computational Physics, University of Coimbra, 3004-516 Coimbra, Portugal
[f] Faculty of Mathematics and Physics, University of Ljubljana, 1000 Ljubljana, Slovenia

Abstract. The K-matrix approach is applied to the calculation of the multipole amplitudes M_{1+}, E_{1+}, and S_{1+} in the Δ channel within the Cloudy Bag Model. The separation of the amplitudes into the resonant part and the background is presented and discussed.

1 Introduction

In our previous work [1] (see also [2]) we presented a method to calculate pion electroproduction amplitudes in the framework of chiral quark models. We derived the expressions for the transition K-matrix and the T-matrix and showed how to separate the resonant part from the background. In the present work we apply this method to the calculation of amplitudes M_{1+}, E_{1+}, and S_{1+} in the $\Delta(1232)$ channel.

We use the Cloudy Bag Model as a simple example of a chiral quark model. In spite of the known limitations of the model we show that it is possible to reproduce these amplitudes sufficiently well in a broad energy range. We explain how to isolate the resonant parts of the amplitudes and show that these parts are in good agreement with the results extracted from the experiment.

2 Electro-production amplitudes and cross-sections

In electro-production, the incoming virtual photon with four-momentum $(\omega_\gamma, \mathbf{k}_\gamma)$, $\omega_\gamma^2 - \mathbf{k}_\gamma^2 = -Q^2$, and polarization μ interacts with the nucleon with the third components of spin m_s and isospin m_t; the final state consists of the scattered pion with four-momentum $(\omega_0, \mathbf{k}_0)$ and the third component of isospin t and the nucleon with good m_s' and m_t'. In the c.m. frame the nucleon momentum is opposite to that of the photon (pion). If the z-axis is oriented in the direction of the incoming photon, the K-matrix for this process can be written as

$$K_{\gamma\pi} = -\pi\langle\Psi^P(m_s, m_t; \mathbf{k}_0, t)|H_\gamma|N(m_s', m_t'); \mathbf{k}_\gamma, \mu\rangle \ . \qquad (1)$$

* Talk delivered by B. Golli

Here Ψ^P is a *principal-value* state (see e.g. [3]) while $|N(m_s', m_t'); \mathbf{k}_\gamma, \mu\rangle$ stands for the asymptotic (free) states representing the nucleon and the photon. The principal value state can be written in the form[1]:

$$|\Psi^P\rangle = \sqrt{\frac{\omega_0}{k_0}} \left\{ a_t^\dagger(\mathbf{k}_0)|N(m_s, m_t)\rangle + \int d\mathbf{k} \, \frac{\chi(k_0, k)}{\omega_k - \omega_0} a_t^\dagger(\mathbf{k})|N(m_s, m_t)\rangle + c_R|R\rangle \right\} , \tag{2}$$

where $a_t^\dagger(\mathbf{k})$ is the pion creation operator, $|N\rangle$ is the nucleon state, and $|R\rangle$ is a (possible) resonant state with excited internal degrees of freedom (e.g. quarks and/or mesons). The amplitude describing the scattered pion, $\chi(k_0, k)$, is related to the phase shift. The state (2) is normalized as

$$\langle \Psi_\alpha^P(E)|\Psi_\beta^P(E')\rangle = (1 + K^2)_{\alpha\alpha} \, \delta(E - E')\delta_{\alpha\beta} , \tag{3}$$

where E is the total energy of the system K is the K-matrix for pion scattering, and α, β label different channels. The normalization (3) is not practical in numerical calculations because the factor in front of the δ function diverges as E approaches the resonant energy. It is more convenient to work with the state normalized simply to $\delta(E - E')$ at the resonance:

$$|\Psi_R\rangle = K_{\pi\pi}^{-1}|\Psi^P\rangle . \tag{4}$$

We now expand Ψ^P (or equivalently Ψ_R) in (1) in states with good total angular momentum J and isospin T:

$$\begin{aligned} K_{\gamma\pi} = K_{\pi\pi}\sqrt{\omega_\gamma k_\gamma} \sum_{lm} \langle \Psi_R J, T, M_J M_T; k_0, l|[H_\gamma \, , a_\mu^\dagger(\mathbf{k}_\gamma)]|N(m_s', m_t')\rangle \\ \times Y_{lm}(\vartheta, \varphi) C^{JM_J}_{\frac{1}{2}m_s lm} C^{TM_T}_{\frac{1}{2}m_t 1t} + \dots , \end{aligned} \tag{5}$$

where ϑ is the angle between the scattered pion and the incident photon, $a_\mu^\dagger(\mathbf{k}_\gamma)$ is the creation operator for the photon, the factor $\sqrt{\omega_\gamma k_\gamma}$ ensures the proper normalization of the photon asymptotic state, and C's are the Clebsh-Gordan coefficients. Since we are usually interested in one particular channel with given J and T we have denoted by $\dots$ other channels not taken into account.

The T-matrix is obtained as

$$T_{\gamma\pi} = K_{\gamma\pi}(1 + iT_{\pi\pi}) , \tag{6}$$

yielding a similar expression as (5) in which $K_{\pi\pi}$ is replaced by $T_{\pi\pi}$. The appearance of $K_{\pi\pi}$ ($T_{\pi\pi}$) in front of the (real) transition amplitude means that the phase shift of the transition K or T-matrix is that of the meson scattering – an explicit manifestation of the Watson theorem. In fact, in the above derivations, we have tacitly assumed that "switching on" the electro-magnetic interaction H_γ does not change the strong scattering amplitudes, i.e. the principal-value state (2) remains unchanged.

[1] Here the normalization of the principal value state (see (3)) and consequently the definition of the K-matrix is changed slightly with respect to the ones used in [1].

To obtain the electro-production amplitudes in the Δ-channel, we keep only the p-wave pions and the $J = T = \frac{3}{2}$ component of the final state in (5); we furthermore neglect nucleon recoil and the effect of the two-pion decay channel. The pertinent electro-production amplitudes are related to the matrix elements of the T-matrix, by

$$M_{1+}^{(3/2)} = T_{\pi\pi}\sqrt{\frac{3}{16k_0k_\gamma}}\,\frac{1}{\pi}\,\left[-\frac{1}{2\sqrt{3}}\,(3K_{3/2}+\sqrt{3}K_{1/2})\right] \tag{7}$$

and

$$E_{1+}^{(3/2)} = T_{\pi\pi}\sqrt{\frac{3}{16k_0k_\gamma}}\,\frac{1}{\pi}\,\frac{1}{2\sqrt{3}}\,(K_{3/2}-\sqrt{3}K_{1/2})\,. \tag{8}$$

Here we have introduced the analogues of the familiar helicity amplitudes:

$$K_\lambda = \sqrt{\omega_\gamma k_\gamma}\,\langle\Psi_R(M_J=\lambda)|\frac{e_0}{\sqrt{2\omega_\gamma}}\int d\mathbf{r}\,\boldsymbol{\varepsilon}_\mu\cdot\mathbf{j}(\mathbf{r})e^{i\mathbf{k}_\gamma\cdot\mathbf{r}}|N(m_s'=\lambda-\mu)\rangle\,, \tag{9}$$

where $\mathbf{j}(\mathbf{r})$ is the vector part of the electro-magnetic current. The differential cross section then reads

$$\frac{d\sigma_T}{d\Omega} = \frac{k_0}{k_\gamma}\left\{\frac{1}{2}\,|M_{1+}|^2(5-3\cos^2\vartheta)+\frac{9}{2}\,|E_{1+}|^2(1+\cos^2\vartheta)\right.$$
$$\left.+\,3\mathrm{Re}M_{1+}^*E_{1+}(1-3\cos^2\vartheta)\right\}\,.$$

The longitudinal amplitude is

$$L_{1+}^{(3/2)} = T_{\pi\pi}\sqrt{\frac{3\omega_\gamma}{32\pi^2k_0}}\,\langle\tilde{\Psi}(M_J=\tfrac{1}{2})|\frac{e_0}{\sqrt{2\omega_\gamma}}\int d\mathbf{r}\,\boldsymbol{\varepsilon}_0\cdot\mathbf{j}(\mathbf{r})e^{i\mathbf{k}_\gamma\cdot\mathbf{r}}|N(m_s'=\tfrac{1}{2})\rangle\,, \tag{10}$$

with

$$\frac{d\sigma_L}{d\Omega} = \frac{k_0}{k_\gamma}\,|L_{1+}|^2\left\{4+12\cos^2\vartheta\right\}\,. \tag{11}$$

3 Calculation of the K-matrix in chiral quark models

We consider quark models in which the p-wave pions couple to the three-quark core. Assuming a pseudo-scalar interaction, the pion part of the Hamiltonian is

$$H_\pi = \int dk\sum_{mt}\left\{\omega_k\,a_{mt}^\dagger(k)a_{mt}(k)+\left[V_{mt}(k)a_{mt}(k)+V_{mt}(k)^\dagger\,a_{mt}^\dagger(k)\right]\right\}\,, \tag{12}$$

where $a_{mt}^\dagger(k)$ is the creation operator for a p-wave pion with the third components of spin m and isospin t, and $V_{mt}(k) = -V(k)\sum_{i=1}^3\sigma_m{}^i\tau_t{}^i$ represents the general form of the pion source in which the function $V(k)$ depends on the particular model. In the Cloudy Bag Model, $V(k)$ reads

$$V(k) = \frac{k^2}{\sqrt{12\pi^2\omega_k}}\,\frac{\omega_{MIT}^0}{\omega_{MIT}^0-1}\,\frac{j_1(kR)}{2f_\pi kR}\,, \tag{13}$$

where $\omega_{MIT}^0 = 2.0428$. The free parameters are the bag radius R and the energy splitting between the bare nucleon and the bare delta which is adjusted such that the experimental position of the resonance is reproduced.

Neglecting recoil, $\omega_\gamma = \omega_0 = E - E_N$, the trial state takes the form

$$|\Psi\rangle = \sqrt{\frac{\omega_0}{k_0}} \left\{ \left[a^\dagger_{mt}(k_0)|\Phi_N\rangle \right]^{\frac{3}{2}\frac{3}{2}} + \int dk\, \frac{\chi(k,k_0)}{\omega_k - \omega_0} \left[a^\dagger_{mt}(k)|\Phi^E_N\rangle \right]^{\frac{3}{2}\frac{3}{2}} + c^E_\Delta |\Phi_\Delta\rangle \right\} . \tag{14}$$

Here Φ_Δ denotes the resonant state representing the bare delta (i.e. three quarks in s-state coupled to $J = T = \frac{3}{2}$) and a cloud of up to two pions around the bare nucleon and delta.

The pion profiles in Φ_N and Φ_Δ can be most easily determined from the following relations that hold for Hamiltonians of the type (12):

$$a_{mt}(k)|A\rangle = -\frac{V^\dagger_{mt}(k)}{\omega_k + H - E_A}|A\rangle \tag{15}$$

and

$$a_{mt}(k)a_{m't'}(k')|A\rangle = \frac{V^\dagger_{mt}(k)}{\omega_k + \omega'_k + H - E_A}\ \frac{V^\dagger_{m't'}(k')}{\omega'_k + H - E_A}|A\rangle + [k \leftrightarrow k'] , \tag{16}$$

where $|A\rangle$ is an eigenstate of H; in our case either $|\Phi_N\rangle$ or $|\Psi\rangle$.

From (14) we have calculated the P33 phase shift as well as the multipole amplitudes for the electroproduction. In order to reproduce the experimental phase shift (see Fig. 1) we had to reduce the value of the pion decay constant appearing in (13) from the experimental value 93 MeV to $83\,\text{MeV} > f_\pi > 78\,\text{MeV}$ for $0.9\,\text{fm} < R < 1.1\,\text{fm}$, respectively.

As seen from Figs. 2 the experimental values for the electroproduction amplitudes are underestimated. The reason lies in a too weak $\gamma N\Delta$ vertex, which is a known feature of the Cloudy Bag Model. Taking a smaller R and reducing further the value of f_π [4] enhances the contribution of the pion cloud, and thus increases the strength of the $\gamma N\Delta$ vertex. Yet this mechanism does not help to improve the agreement: increasing the strength of the quark-pion interaction leads to a larger width of the resonance, and since $\sqrt{\Gamma}$ appears (implicitly) in the denominator of the amplitudes (9) and (10), the net effect is such that the magnitude of the $\text{Im}\, M_{1+}$ in the vicinity of the resonance *decreases*.

4 Extracting the resonance

In some models, the delta resonance is described as a particle with a finite lifetime and an energy corresponding to the pole of the T-matrix in the complex energy plane. The properties of such a particle can not be directly related to the measured amplitudes since the amplitude include also non-resonant processes. In this section we show how to relate the results obtained in the K-matrix approach to those of the above mentioned models.

The resonant part of the amplitudes is usually assumed to have a Breit-Wigner shape with a constant width (see Eq. (18)) below). In order to identify

the part in the total amplitude that possesses this type of behavior we write the pertinent K-matrix in the form proposed in [5]:

$$K_{\pi\pi} = \frac{C}{E_\Delta - E} + D\,, \tag{17}$$

with two constant coefficients C and D. Using these two parameters and the experimental value for E_Δ we obtain an excellent fit to the calculated phase shift (see Fig. 1). The corresponding T-matrix can be cast in the form, suggested by Wilbois et al. in the speed-plot analysis (Eqs. (71)-(76) of [6]):

$$T_{\pi\pi} = \frac{K_{\pi\pi}}{1 - iK_{\pi\pi}} = e^{2i\delta_b}\,\frac{\Gamma_\Delta^T/2}{M_\Delta - E - i\Gamma_\Delta^T/2} + \sin\delta_b e^{i\delta_b}\,. \tag{18}$$

The parameters of the T-matrix can be easily deduced from (17) and are given in Table 1. Since we started from a real K-matrix, the resulting T-matrix automatically obeys unitarity, which is an important merit of our approach.

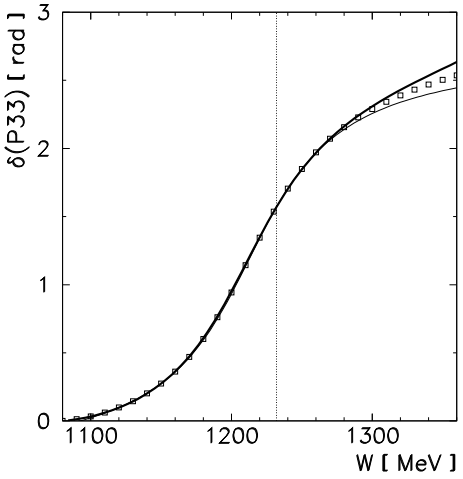

Fig. 1. The phase shift in the P33 channel as a function of the invariant mass. The data points are the single-energy values of the SM02K (2GeV) solution of the SAID πN partial-wave analysis [7]. The thick line represents the calculated phase shift, while the thin line is the two-parameter fit to the calculated values. The agreement is worse only above 1300 MeV where the two-pion channel becomes relevant and our approach is not valid anymore.

In a similar way we can split the K-matrix for the electroproduction in the resonant and the background part:

$$K_{\gamma\pi} = \frac{A}{E_\Delta - E} + B\,. \tag{19}$$

The parameters A and B for each multipole can be determined by fitting the calculated amplitudes using the form implied by (7) and (8):

$$\mathcal{M} = \frac{1}{\sqrt{k_0 k_\gamma}}\,\frac{K_{\gamma\pi}}{1 - iK_{\pi\pi}}\,, \tag{20}$$

where $\mathcal{M}$ is ether $M_{1+}^{(3/2)}$ or $E_{1+}^{(3/2)}$. Alternatively, one can use a simplified form:

$$\mathcal{M} = \frac{K_{\gamma\pi}}{1 - iK_{\pi\pi}}\,, \tag{21}$$

which is more frequently used in the experimental analysis, e.g. in [8] and in the SP-analysis of [6]; the form (20) being used in the MSP analysis of [6]. The resulting parameters are listed in Table 1.

Table 1. Resonance pole parameters extracted from the computed phase shifts and electro-production amplitudes using the form (21). Parameter C is the resonance width divided by 2, D is the tangent of the background phase shift, and M_Δ and Γ_Δ^T are parameters of the T-matrix (see (18)). Experimental values are the recent PDG values [9] and from [6].

R	f_π	C	D	M_Δ	Γ_Δ^T	A(M1)	B(M1)	A(E2)	B(E2)
[fm]	[MeV]	[MeV]		[MeV]	[MeV]		$[10^{-3}/m_\pi]$		$[10^{-3}/m_\pi]$
1.1	78	57	−0.39	1213	49	0.0123	−2.57	−0.000235	−1.19
1.0	81	56	−0.40	1213	48	0.0117	−3.53	−0.000236	−1.09
0.9	83	56	−0.41	1212	48	0.0115	−4.00	−0.000221	−1.00
Experiment		60	−0.435	1210	50				

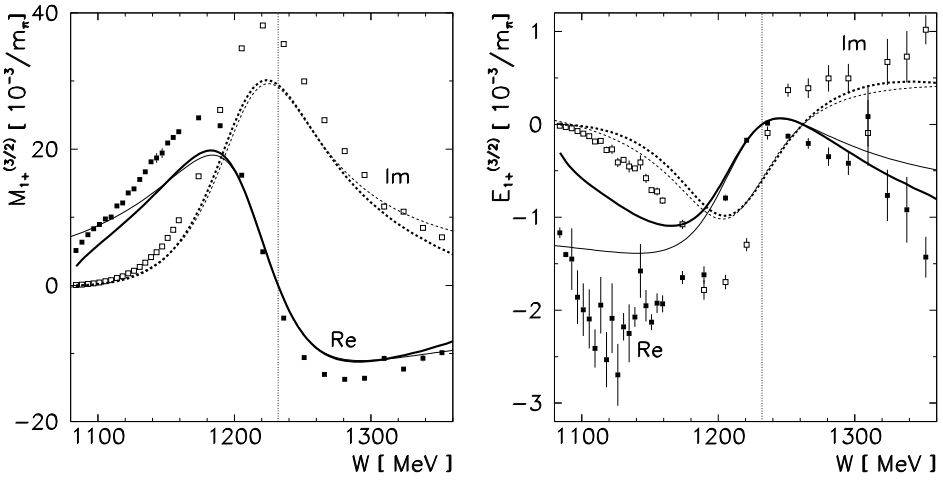

Fig. 2. The $M_{1+}^{(3/2)}$ and the $E_{1+}^{(3/2)}$ electro-production amplitude in the CBM by using $R = 1.0$ fm and $f_\pi = 81$ MeV. The data points in the figures are the single-energy values of the SM02K (2 GeV) solution of the SAID πN partial-wave analysis [7]. The thick lines represent the calculated amplitudes for $R = 1.0$ fm and $f_\pi = 81$ MeV, while the thin lines are the fits to the calculated values using the parameters from Table 1.

From our results it is possible to extract the resonance parameters at the pole of the T-matrix, based on the separation of the amplitude into the resonant and

background parts, using the parameterization [6,8]

$$T = T_R + T_B\,, \qquad T_R = \frac{r\Gamma_\Delta^T e^{i\phi}}{M_\Delta - E - i\Gamma_\Delta^T/2}\,. \tag{22}$$

Using (20), the parameters r, ϕ, and T_B can be expressed in terms of A, B, C, and D. The moduli and phases for the transverse multipoles are shown in Table 2 together with the EMR ratio. While the magnitudes are underestimated, the ratio as well as the phases are much better reproduced.

Table 2. Resonance pole parameters extracted from the computed $E_{1+}^{(3/2)}$ and $M_{1+}^{(3/2)}$ multipoles using the form (21) and parameters in Table 1, compared to various determinations from data. The moduli r are in units of $10^{-3}/m_\pi$. R_Δ is the EMR ratio at the pole of the T-matrix.

R [fm]$/f_\pi$ [MeV]	r_E	ϕ_E	r_M	ϕ_M	R_Δ
1.1 / 78	0.75	$-154°$	16	$-25°$	$-0.031 - 0.037\,i$
1.0 / 81	0.72	$-158°$	15	$-28°$	$-0.030 - 0.037\,i$
0.9 / 83	0.67	$-159°$	14	$-31°$	$-0.029 - 0.037\,i$
Ref. [8]	1.23	$-154.7°$	21.2	$-27.5°$	$-0.035 - 0.046\,i$
Ref. [6] (SP)	1.23	$-156°$	19.9	$-26.0°$	$-0.040 - 0.047\,i$
Ref. [10], Fit 1	1.22	$-149.7°$	22.2	$-27.4°$	$-0.029 - 0.046\,i$
Ref. [11], Fit A	1.38	$-158°$	20.9	$-31°$	$-0.040 - 0.053\,i$

Table 3. Same as Table 2 except that the parameterization (20) is used.

R [fm]$/f_\pi$ [MeV]	r_E	ϕ_E	r_M	ϕ_M	R_Δ
1.1 / 78	0.74	$-157°$	16	$-34°$	$-0.026 - 0.038\,i$
1.0 / 81	0.68	$-160°$	15	$-37°$	$-0.025 - 0.037\,i$
0.9 / 83	0.62	$-162°$	14	$-40°$	$-0.023 - 0.037\,i$
Ref. [6] (MSP)	1.12	$-162°$	20.7	$-36.5°$	$-0.032 - 0.044\,i$

5 Discussion

We have presented a method to calculate directly the K-matrices of resonant electro-production processes in the framework of chiral quark models.

The identification of the resonant part and the background is unambiguous in the K-matrix formalism. In the T-matrix formalism, this separation is based on

the assumption that the position and the width of the resonance do not depend on the invariant energy and is intimately connected to our picture of a resonance as a short-lived particle. While such an assumption cannot be justified in a microscopic model, it is surprising how well it reproduces the experimental results in a broad range of energies. (The agreement at low and high energies in Fig. 2 can be improved by assuming that the background part is energy-dependent.)

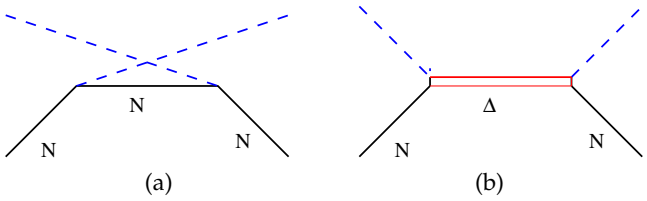

Fig. 3. Two processes dominating the P33 channel

Neither the resonant part nor the background are related to a specific process, such as those depicted in Fig 3. Naively, one would expect that graph (b) corresponds to the resonant part and graph (a) to the background. Yet they both contribute to the resonant part as well as to the background; note that the process (a) alone can lead to the resonance in this channel for sufficiently strong πN coupling and has the opposite sign with respect to the background contribution in the whole energy range.

Let us conclude by noting that a good microscopic model should be able to reproduce the *total* amplitude and not just the resonant part, since, as seen from Tables 2 and 3, the extracted values from the experiment are too unreliable to serve as benchmarks.

References

1. B. Golli, in: B. Golli, M. Rosina, S. Širca (eds.), *Proceedings of the Mini-Workshop "Effective Quark-Quark Interaction*, July 7–14, 2003, Bled, Slovenia, p. 83.
2. P. Alberto, L. Amoreira, M. Fiolhais, B. Golli, S. Širca, submitted to Phys. Lett. B, hep-ph/0409246.
3. R. G. Newton, *Scattering Theory of Waves and Particles*, Dover Publications, New York 1982.
4. K. Bermuth, D. Drechsel, L. Tiator, J. B. Seaborn, Phys. Rev. D **37** (1988) 89.
5. R. M. Davidson, N.C. Mukhopadhyay, Phys. Rev. D **42** (1990) 20.
6. Th. Wilbois, P. Wilhelm, H. Arenhövel, Phys. Rev. C **57** (1998) 295.
7. R. A. Arndt, W. J. Briscoe, R. L. Workman, I. I. Strakovsky, SAID Partial-Wave Analysis, `http://gwdac.phys.gwu.edu/`.
8. O. Hanstein, D. Drechsel, L. Tiator, Phys. Lett. B **385** (1996) 45.
9. S. Eidelman et al., Phys. Lett. B **592** (2004) 1.
10. R. M. Davidson et al., Phys. Rev. C **59** (1999) 1059; the average of VPI and RPI analysis results is listed.
11. R. Workman, R. A. Arndt, Phys. Rev. C **59** (1999) 1810.